MicroRNA-1285 Regulates 17β-Estradiol-Inhibited Immature Boar Sertoli Cell Proliferation via Adenosine Monophosphate-Activated Protein Kinase Activation

Zhang Jiao Jiao, Wang Yi, Yang Wei Rong, Jeong Dong Kee, and Wang Xian Zhong

Chongqing Key Laboratory of Forage and Herbivore (Z.J.J., W.Y., Y.W.R., W.X.Z.), College of Animal Science and Technology, Southwest University, Chongqing 400715, China; and Genetic Engineering and Stem Cell Biology Laboratory (Z.J.J., J.D.K.), Department of Animal Biotechnology, Faculty of Biotechnology, Jeju National University, Jeju 690756, South Korea

This study investigated the capacity of 10 μM 17β-estradiol to inhibit immature boar Sertoli cell (SC) proliferation and the involvement of microRNA (miR)-1285 in this process. SC viability and cell cycle progression were investigated using a cell counting kit-8 and flow cytometry, respectively. Expression of AMP-activated protein kinase (AMPK), S phase kinase-associated protein 2 (Skp2), and miR-1285 was analyzed by real-time RT-PCR and Western blotting. 17β-Estradiol (10 μM) reduced SC viability and miR-1285 expression and promoted AMPK phosphorylation. A double-stranded synthetic miR-1285 mimic promoted SC viability, increased levels of ATP, and phosphorylated mammalian target of rapamycin (mTOR) and *Skp2* mRNA and protein, whereas p53 and p27 expression decreased, and 17β-estradiol-mediated effects on SCs were significantly attenuated. A single-stranded synthetic miR-1285 inhibitor produced the opposite effects on these measures. Activation of AMPK inhibited SC viability, reduced levels of ATP, phosphorylated mTOR and *Skp2* mRNA and protein, and increased p53 and p27 expression. An AMPK inhibitor (compound C) attenuated the effects of 17β-estradiol on SCs. This indicated that 17β-estradiol (10 μM) reduced SC proliferation by inhibiting miR-1285 and thus activating AMPK. Phosphorylated AMPK is involved in the regulation of 17β-estradiol-mediated inhibition of SC viability through increasing p53 and p27 expression and inhibiting mTOR and Skp2 expression. Our findings also implicated Skp2 as the downstream integration point of p53 and mTOR. These findings indicated that miR-1285 may represent a target for the manipulation of boar sperm production. **(*Endocrinology* 156: 4059–4070, 2015)**

Sertoli cells (SCs) play a vital role in spermatogenesis by providing support and nutrition for spermatogenic cells. During spermatogenesis, lactate is the preferred substrate of spermatocytes and spermatids. Lactate production from glucose in SCs is an important point for the control of spermatogenesis (1). SCs also secrete proteins and cytokines, which participate in the control of sperm movement from the testis to the epididymis and in the control of the pH of the seminiferous fluid (2). Furthermore, adjacent SCs form the blood-testis barrier, which inhibits the entry of molecules exceeding 1000 Da into the seminiferous tubule. This barrier also prevents autoimmunity and maintains a stable microenvironment for germ cell differentiation (3).

ISSN Print 0013-7227 ISSN Online 1945-7170
Printed in USA

Received December 8, 2014. Accepted August 14, 2015.
First Published Online August 19, 2015

Abbreviations: AICAR, 5-aminoimidazole-4-carboxamide ribonucleoside; AMPK, AMP-activated protein kinase; dH_2O, distilled H_2O; miRNA, micro-RNA; miR-1285 inhibitor, chemically modified single-stranded RNA with a base sequence complementary to miR-1285; miR-1285 inhibitor NC, miR-1285 inhibitor negative control; miR-1285 mimic NC, miR-1285 mimic negative control; mTOR, mammalian target of rapamycin; p, phosphorylated; PI, proliferation index; RNase, ribonuclease; SC, Sertoli cell; S6K, S6 protein kinase; Skp2, S-phase kinase-associated protein 2; SPF, S phase index; TE, transposable element; UTR, untranslated region.

Each SC provides support to a limited number of differentiating germ cells, with the number of SCs in adult animals determining the size of the testis and the competence of spermatogenesis. SC viability and proliferation indices reflect cell proliferation capacity, which is a vital determinant of cell number. Boar exhibit two phases of SC proliferation after birth; these occur from birth to 1 month old and from 3–4 months until puberty (4). The proliferation of SCs is regulated by hormones and growth factors, with estrogens playing an important role in this process (5). Estrogens have been shown to stimulate synthesis of TGF-β and DNA by SCs, increasing their proliferation (6). A reduction in the levels of prepubertal endogenous estrogens was shown to increase the SC number in boars, resulting in increasing testicular size and testicular sperm production capacity (7). Moreover, reducing both perinatal and peripubertal levels of endogenous estrogens increased the number of SCs, and a continuous reduction of the estrogens levels maintained this increase, without affecting the fertilization capacity of boar sperm (8). An intratesticular concentration of estradiol of 200 μg/kg·d, which was more than 10 times higher than normal levels, reduced the expression of proliferative cell nuclear antigen in SCs, inhibited SC proliferation, and increased SC and germ cell apoptosis in immature rats during puberty (9). Our previous research showed that low doses of 17β-estradiol (0.0001–0.1 μM) increased the number of immature boar SCs, whereas a higher dose (1 μM) reduced the number of SCs (10). These conflicting results suggest that 17β-estradiol has both positive and negative effects on SC proliferation.

Mammalian cell proliferation is negatively regulated by cyclin-dependent kinase inhibitors and tumor suppressor genes. The cyclin-dependent kinase inhibitor, $p27^{KIP1}$ (p27), inhibits cell proliferation by reducing cyclin/cyclin-dependent kinase activity and the phosphorylation of retinoblastoma tumor suppressor protein; this causes G_1 arrest. The tumor suppressor, p53, inhibits the cell cycle indirectly by promoting p27 transcription (11). S-phase kinase-associated protein 2 (Skp2), which is a key protein involved in regulating the cell cycle, promotes the degradation of p27. Mammalian target of rapamycin (mTOR) influences cell cycle progression and cell proliferation by increasing the expression of ribosomal S6 protein kinases (S6K) and transcription initiation factor 4E binding protein 1 (12, 13). AMP-activated protein kinase (AMPK) plays a role in cellular energy homeostasis and cell proliferation by regulating the expression of genes involved in these processes. AMPK inhibits the proliferation of hepatocellular carcinoma cells (14), mouse embryonic fibroblasts (15), human aortic smooth muscle cells, rabbit aortic strips (16), osteosarcoma cells (17), and glioblastoma (18). The AMPK activator, 5-aminoimidazole-4-carboxamide ribonucleoside (AICAR), inhibits the activation of S6K in human corneal epithelial cells infected with sarcoma virus 40 (19). Activated AMPK regulates cell proliferation by regulating mTOR phosphorylation. Furthermore, AMPK increases the expression of p53 and p27 proteins, inhibiting the proliferation of cancer cells both in vitro and in vivo (20) via phosphorylation of p53 at Ser15 (21). However, it is unclear whether 17β-estradiol activates AMPK to reduce boar SC proliferation by inhibiting the mTOR signaling pathways and regulating the expression of p53, p27, and Skp2.

Micro-RNAs (miRNAs) play important roles in cell proliferation, differentiation, apoptosis, and tumorigenesis by mediating RNA silencing and regulating gene expression at the posttranscriptional level (22). Some miRNAs are processed from transposable elements (TE)-derived loci, and TE-derived miRNAs can regulate target mRNAs through complementary target sites located within 3′ untranslated region (UTR)-resident TE homologs (23, 24). MiR-1285 was first discovered from massively parallel sequencing of human embryonic stem cells (25). Alu-derived miR-1285–1 was efficiently processed from its genomic locus and found to regulate genes with target sites within homologous elements; overexpression of a miR-1285–1 mimics a significantly reduced expression of three luciferase reporters with Alu-derived target sites (26). Our previous study showed that a chemically modified double-stranded RNA that mimics miR-1285 and enables miR-1285 functional analysis by the up-regulation miR-1285 activity (miR-1285 mimic) directly down-regulated the expression of AMPK induced by AICAR via a 3′ UTR target site (Zhang J.J., Wang Y., Yang W.R., Jeong D.K., Wang X.Z., unpublished data). Therefore, we hypothesized that miR-1285 regulates the 17β-estradiol-mediated inhibition of immature boar SC proliferation via effects on AMPK activation. The present study was designed to examine whether 17β-estradiol inhibited cultured immature boar SC proliferation and to explore the potential involvement of miR-1285 in this process. Furthermore, the effects of AMPK activation on the expression of mTOR, p53, p27, and Skp2 were also investigated.

Materials and Methods

Chemicals

DMEM/F-12, Lipofectamine 2000 transfection reagent, and Opti-MEM were purchased from Invitrogen. Collagenase VI, penicillin and streptomycin, dimethyl sulfoxide, compound C, and 17β-estradiol were obtained from Sigma-Aldrich. Trypsin

was obtained from Amresco LLC. AICAR was purchased from Biomol.

Culture of boar SCs

Testes were obtained under sterile conditions from immature boars (Landrace, aged 21 d) raised at a local livestock farm (Beibei, Chongqing). All experiments involving animals were conducted in accordance with the Regulations for the Administration of Affairs Concerning Experimental Animals (Ministry of Science and Technology, China, revised in June 2004) and approved by the Institutional Animal Care and Use Committee in Southwest University (China). SCs were isolated from the testes, evaluated for purity, and cultured using previously described methods (10, 27). After collection, centrifugation for 5 minutes at 1000 × *g*, and resuspension, 2×10^5 cells/mL, were cultured in 25-cm^2 culture bottles in a humidified atmosphere containing 5% CO_2 at 32°C with DMEM/F-12 (1:1) basic medium containing l-glutamine (10 μg/mL), 15 mM HEPES, 5% fetal bovine serum (Gibco-Invitrogen), streptomycin (20 μg/mL), penicillin (20 μg/mL), and tocopherol (10 μg/mL). After 12 hours, residual germ cells were removed as previously described (10, 27). SCs were cultured for approximately 48 hours to 70%–80% confluence prior to use in experiments.

Analysis of cell viability and cell cycle progression

For cell viability assays, 2×10^5 cells/mL were plated in 96-well plates and cultured. At 70%–80% confluence, immature boar SCs were either exposed to compound C (40 μM) only for 24 hours or to compound C only for 18 hours, followed by 17β-estradiol (10 μM) and compound C for 6 hours. SCs were also exposed to either AICAR (2 mM) or 17β-estradiol for 6 hours before analysis, whereas control cells were treated with vehicle (isometric dimethyl sulfoxide) for 24 hours. Cell viability was detected with a cell counting kit-8 (Dojindo Molecular Technologies), as previously described (10, 28). Briefly, a calibration curve was constructed using suspensions of known numbers of SCs. The cell counting kit-8 solution (10 μL/well) was added and the plates were incubated for 1 hour. Absorbance was measured at 450 nm using a microplate reader (Bio-Rad Co). SC viability (percentage) was calculated by the following equation: (absorbance of treatment group − absorbance of blank)/(absorbance of control group − absorbance of blank) × 100%.

SCs (2×10^5 cells/mL) were seeded in 25-cm^2 culture bottles containing DMEM/F-12 culture medium and cultured for 4 days before cell cycle analysis. SCs were washed with ice-cold PBS, centrifuged (200 × *g*) for 5 minutes at 4°C, resuspended in ice-cold PBS, and fixed in ice-cold 70% ethanol for 24 hours. They were then centrifuged for 10 minutes (200 × *g*) at 4°C, digested with 50 μg/mL ribonuclease (RNase)-A for 15 minutes at 37°C, and stained with 50 μg/mL propidium iodide for 30 minutes at 4°C, protected from light. The cell cycle was analyzed by measuring the DNA content using a fluorescence-activated cell sorter (Cytomics FC500; Beckman Coulter), and ModFit LT (Macintosh) was used to assign each cell to a particular stage in the cell cycle. The numbers of cells in G_0/G_1, S, and G_2/M phases were determined and reported as the proliferation index (PI) and S phase index (SPF), where $PI = (S + G_2/M)/(G_0/G_1 + S + G_2/M) \times 100\%$, and $SPF = S/(G_0/G_1 + S + G_2/M) \times 100\%$.

Transfections

SCs (2×10^5 cells/mL) were seeded in 25-cm^2 culture bottles with 3 mL Opti-MEM. At 30%–50% confluence, the SCs were mock transfected (Lipofectamine 2000 only; Invitrogen) or transfected with complexes of Lipofectamine 2000 and miR-1285 mimic (50 nM) or miR-1285 mimic negative control (miR-1285 mimic NC; 50 nM) or a chemically modified single-stranded RNA with a base sequence complementary to miR-1285 (miR-1285 inhibitor; 100 nM) or miR-1285 inhibitor negative control (miR-1285 inhibitor NC; 100 nM) (Invitrogen), in the presence or absence of 17β-estradiol (10 μM) for 6 hours, according to the manufacturer's Lipofection protocol. The transfection conditions were optimized in a preliminary experiment (unpublished data). The sequence of the miR-1285 mimic was as follows: 5′-CUGGGCAACAUAGCGAGACCCCGU-3′ and 5′-ACGGGGUCUCGCUAUGUUGCCCAG-3′. The sequence of the miR-1285 inhibitor was as follows: 5′-ACGGGGUCUCGCUAUGUUGCCCAG-3′. The sequence of the miR-1285 mimic NC, which had low homology with all miRNAs in the miRBase, was as follows: 5′-UUCUCCGAACGUGUCACGUTT-3′ and 5′-ACGUGACACGUUCGGAGAATT-3′. The sequence of the miR-1285 inhibitor NC was as follows: 5′-CAGUACUUUUGUGUAGUACAA-3′. The transfected SCs were incubated at 32°C in a humidified atmosphere containing 5% CO_2 for 6 hours. The medium was replaced with Opti-MEM and the cells were incubated for a further 48 hours.

ATP assays

ATP concentrations were determined using a commercially available kit (Beyotime) according to the manufacturer's protocol. SCs were collected and lysed in ATP lysate buffer. After centrifugation (12 000 × *g*, 5 min, 4°C), the concentration of ATP in the supernatant was determined using a standard curve of known ATP concentrations (0, 0.00625, 0.0125, 0.025, 0.05, and 0.1 μmol/L). Relative light unit values were measured using a luminometer (Glomax multidetection system; Promega).

Western blotting

For extraction of total protein, cultured cells were scraped and resuspended in lysis buffer (5 mM phosphate buffer, pH 7.2; 0.1% Triton X-100; 10 mM sodium fluoride; 1 mM phenylmethylsulfonyl fluoride; 1 mg/L chymostatin) prior to centrifugation for 10 minutes at 11 000 × *g*. The protein concentration was determined by a bicinchoninic acid protein assay kit (BCA; Beyotime) using BSA as a standard protein. Proteins were separated by 10% SDS-PAGE and transferred to polyvinylidene fluoride membranes by wet electrophoretic transfer (Bio-Rad Laboratories). After blocking in PBS-Tween 20 containing 5% dried skimmed milk or 3% BSA for 2 hours at room temperature, membranes were incubated with primary detection antibodies raised against AMPK (rabbit, 1:1000; Cell Signaling Technology), phosphorylated AMPK (Thr172) (p-AMPK) (rabbit, 1:1000; Cell Signaling Technology), mTOR (rabbit, 1:2000; Abcam), phosphorylated (p) mTOR (S2448) (rabbit, 1:1000; Abcam), p53 (mouse, 1:1000; Beyotime), p27 (mouse, 1:1000; Beyotime), Skp2 (rabbit, 1:300; Bioss), and β-actin (rabbit, 1:1000; Bioss) at 4°C overnight. After incubation with either goat antirabbit or goat antimouse immunoglobulin G coupled to horseradish peroxidase (1:5000; Bioss) for 2 hours at room temperature, proteins were visualized by enhanced chemilumines-

cence (SuperSignal West Pico; Pierce Biotechnology). Band intensities were quantified using Quantity One software (Bio-Rad Laboratories). The densitometric value of each AMPK, p-AMPK, mTOR, and p-mTOR band was normalized to the β-actin signal in the same sample before calculating the p-AMPK to AMPK and p-mTOR to mTOR ratios. The densitometric value of the p53, p27, and Skp2 signals were also normalized to the relevant β-actin signal.

Real-time RT-PCR analysis of AMPK, Skp2, and miR-1285 expression

Total RNA was extracted and purified from the cultured immature boar SCs using the RNAprep pure cell kit (Tiangen Biotech), following the manufacturer's instructions. RT-PCR analysis of the expression of miRNAs and mRNAs was performed using the SYBR PrimeScript miRNA RT-PCR kit (TaKaRa), the iScript cDNA synthesis kit (Bio-Rad Laboratories), and the SsoAdvanced SYBR Green Supermix (Bio-Rad Laboratories).

For miRNA analyses, first-strand cDNA synthesis and the poly(A) tailing reaction were performed with 1 μL total RNA (1 μg/μL), 10 μL 2 × miRNA reaction buffer mix, 2 μL 0.1% BSA, 2 μL miRNA PrimeScript reverse transcription enzyme mix, and 5 μL RNase-free distilled H_2O (dH_2O), according to the manufacturer's protocol. The reactions were performed at 37°C for 60 minutes followed by enzyme inactivation at 85°C for 5 seconds. RT-PCR was performed with 12.5 μL SYBR premix Ex-TaqII (2 times), 1 μL cDNA, 9.5 μL RNase-free dH_2O, 1 μL Uni-miR quantitative PCR primer, and 1 μL miRNA forward primer using a PerkinElmer multiwell plate system (Bio-Rad Laboratories). The sequences of the primers used were as follows: miR-1285 forward, 5′-CUGGGCAACAUAGCGAGACC-3′; and U6 forward, 5′-CGCAAGGATGACACGCAAAT-3′. The PCR conditions included denaturation at 95°C for 30 seconds, annealing at 56°C for 30 seconds, and extension at 72°C for 30 seconds, and 40 cycles were conducted.

For mRNA analyses, first-strand cDNA synthesis was performed with 1 μL total RNA (1 μg/μL), 4 μL 5 × iScript reaction mix (Bio-Rad Laboratories), 1 μL iScript reverse transcriptase, and 14 μL RNase-free dH_2O, according to the manufacturer's protocol. Reverse transcription was performed at 25°C for 5 minutes, 42°C for 30 minutes, and enzyme inactivation at 85°C for 5 minutes. RT-PCR was performed with 10 μL SsoAdvanced SYBR Green Supermix (Bio-Rad Laboratories), 1 μL cDNA, 7 μL RNase-free dH_2O, 1 μL forward primer, and 1 μL reverse primer using a PerkinElmer multiwell plate system (Bio-Rad Laboratories). The sequences of the primers were as follows: AMPK forward, 5′-ACCAGGACCCTTTGGCAGTT-3′ and reverse, 5′-GAATCAGGTGGGCTTGTTGC-3′; Skp2 forward, 5′-AGATTCCCGACCAGAGTAGCAA-3′ and reverse, 5′-GATGTTCTCACTGTCCACCTCCT-3′; and β-actin forward, 5′-CTAGTTACACACACGCGGCTCT-3′ and reverse, 5′-CATGAATACCCTGCACAGATCG-3′. The PCR conditions included denaturation at 98°C for 2 minutes, annealing at 62.5°C for 30 seconds, and extension at 72°C for 30 seconds, and 40 cycles were conducted. All primer pairs for RT-PCR covered at least one intron.

The cycle threshold value of each sample was determined using triplicate measurements. The equivalent dilution was calculated according to the standard curve and then normalized to the relevant housekeeping gene (*β-actin* for mRNA, *U6* for miRNA). Each PCR was performed in triplicate, and product sequences were confirmed by direct nucleotide sequencing using an ABI PRISM 7700 sequence detector (Applied Biosystems). Relative expression levels were calculated using the $2^{-\delta\delta CT}$ method (29).

Statistical analysis

Experiments were performed in triplicate. Values are expressed as means ± SD. Statistical analyses were performed using the Statistical Package for the Social Sciences (SPSS version 16.0; SPSS). Data were analyzed by a one-way ANOVA and the Fisher's least significant difference method to determine treatment differences. $P < 0.05$ was considered to indicate statistical significance.

Results

Effects of 17β-estradiol on SC viability and p-AMPK levels

Compared with the control, low doses of 17β-estradiol (0.001–0.01 μM) promoted SC viability ($P < .05$-$.01$), whereas 0.1 μM had no significant effect ($P > .05$). At doses of 17β-estradiol exceeding 0.1 μM, SC viability was significantly decreased (48.12% cell viability vs the control at 10 μM, $P < .01$). This effect appeared to be reversible because cell viability recovered to 93.22% of the control level after the removal of this concentration of 17β-estradiol, with no significant difference as compared with the control group. A higher concentration of 17β-estradiol (100 μM) produced a similar effect on SC viability as that observed in the 10-μM group ($P > .05$ for the comparison of cells treated with 10 and 100 μM); however, SC viability did not recover after the withdrawal of 100 μM 17β-estradiol (Figure 1A). Therefore, 10 μM 17β-estradiol was used in the subsequent experiments.

The inhibitory effect of 10 μM 17β-estradiol on SC viability increased gradually as the exposure time increased. Compared with the control group, viability of SCs exposed to 10 μM 17β-estradiol declined significantly after 2 hours ($P < .05$-$.01$), reaching a maximum inhibition at 6 hours (60.7% of the control viability; $P < .01$); no further inhibition was observed when exposure was prolonged beyond 6 hours (Figure 1B). Therefore, 6 hours was considered appropriate for 17β-estradiol treatment of SCs in subsequent experiments. Compared with the control group, 10 μM 17β-estradiol had no significant effect on AMPK phosphorylation in SCs at 1 hour ($P > .05$). However, 17β-estradiol significantly up-regulated AMPK phosphorylation with prolonged exposure ($P < .05$-$.01$); this had increased by 101.75% at 6 hours, as compared with the control cells (Figure 1C).

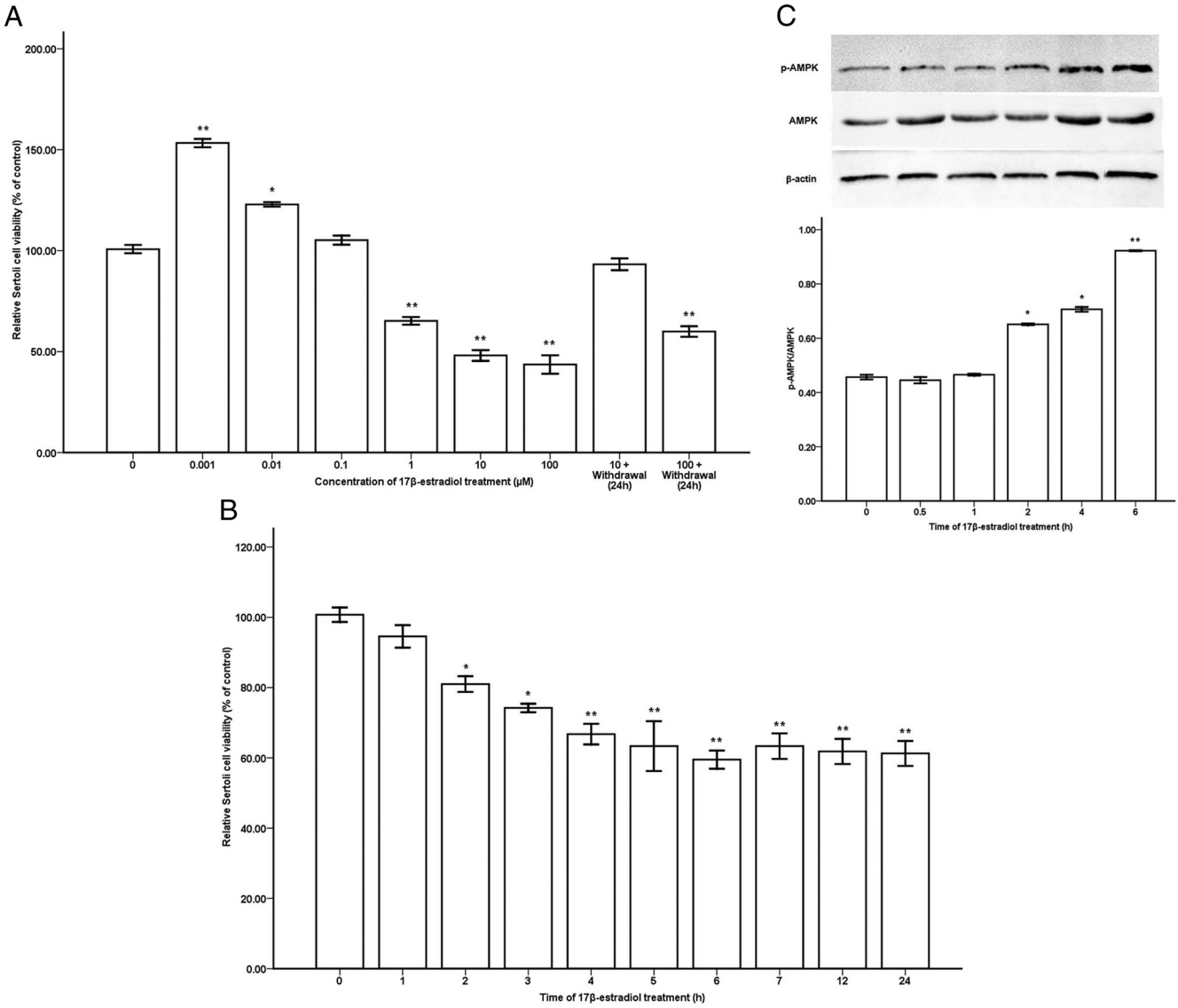

Figure 1. Effects of 17β-estradiol on SC viability and AMPK phosphorylation. A, The viability of immature boar SCs treated with the indicated concentrations of 17β-estradiol for 24 hours. B, Immature boar SCs were treated with 17β-estradiol (10 μM) for the indicated times. Cell viability was detected using a cell counting kit-8. C, Immature boar SCs were incubated with 10 μM 17β-estradiol for the indicated times, and protein was extracted to detect the expression of p-AMPK, AMPK, and β-actin by Western blotting. *, $P < .05$; **, $P < .01$.

Effects of AMPK on 17β-estradiol-regulated SC viability, cell cycle, and expression of miR-1285

Compared with the control, the AMPK activator, AICAR, inhibited SC viability (Figure 2A) and miR-1285 expression (Figure 2C) by 44.74% and 31.51%, respectively (both $P < .01$). AICAR also inhibited cell cycle progression, as reflected by significantly decreased PI and SPF values (by 57.40% and 70.67%, respectively; both $P < .01$) (Figure 2B and Table 1). The AMPK inhibitor, compound C, enhanced SC viability and miR-1285 expression by 23.97% and 36.71%, respectively, as compared with control ($P < .05$-$.01$) (Figure 2, A and C). Compound C also promoted cell cycle progression, with PI and SPF increased by 13.37% and 154.47%, respectively, as compared with the control ($P < .05$-$.01$) (Figure 2B and Table 1). Furthermore, compound C weakened the inhibitory effect of 17β-estradiol on SC viability, cell cycle progression, and miR-1285 expression, with SC viability increased by 56.99% (Figure 2A), with PI and SPF increased by 18.54% and 28.06%, respectively (Table 1), and with miR-1285 expression increased by 15.81% (Figure 2C), as compared with the 17β-estradiol-only group ($P < .05$-$.01$).

Effects of the miR-1285 mimic and inhibitor on 17β-estradiol-regulated expression of miR-1285, SC viability, and cell cycle

Neither negative control produced statistically significant effects as compared with the mock group (Figure 3, A–C, and Table 2) (all $P > .05$). Compared with the mock

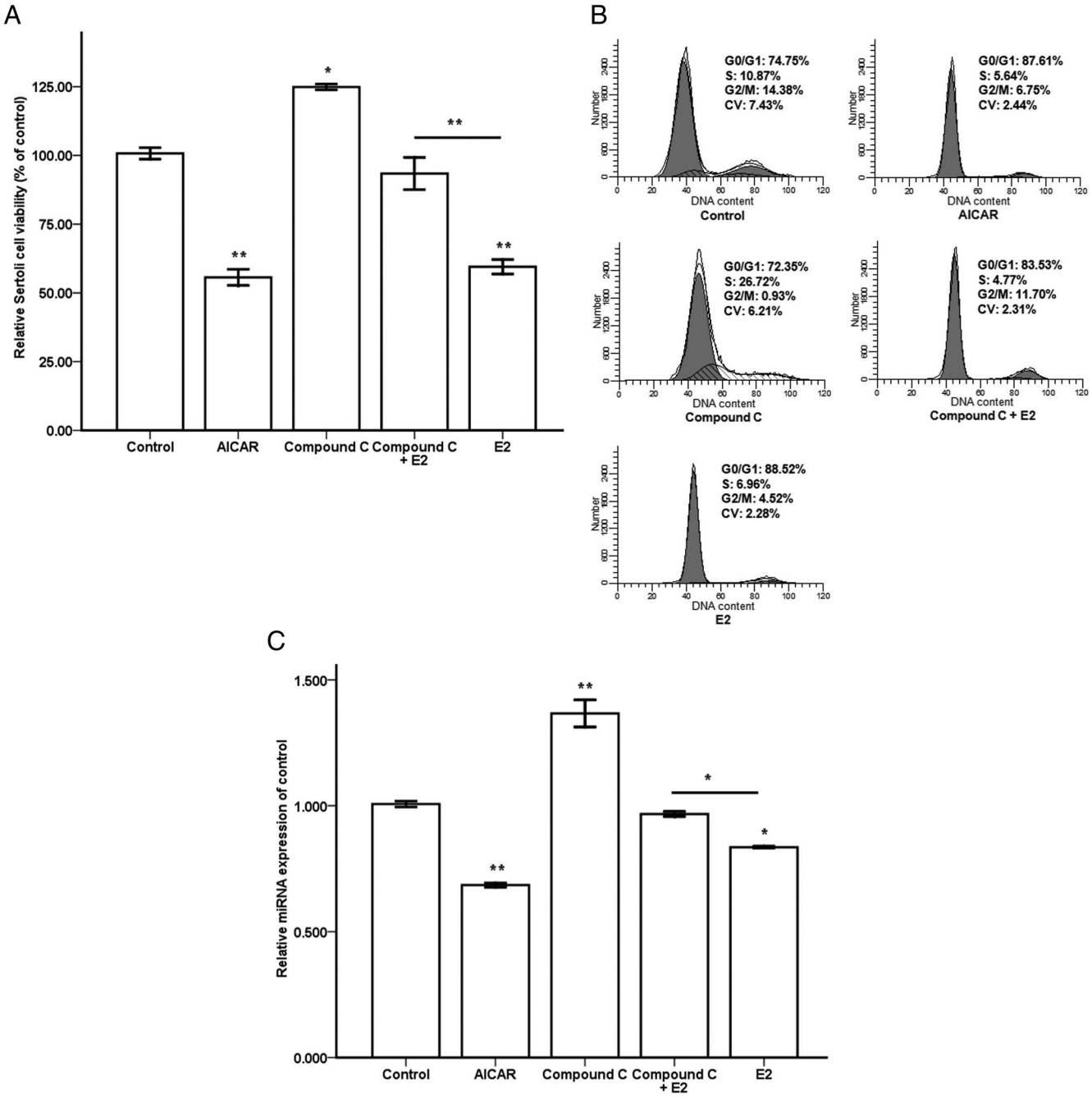

Figure 2. Effects of AMPK on 17β-estradiol-regulated expression of SC viability, the cell cycle, and miRNA (miR)-1285. A, Cell counting kit-8 analysis of SC viability. B, Flow cytometric analysis of the cell cycle. C, Real-time RT-PCR analysis of miR-1285 levels. The expression of miR-1285 was determined in relation to U6 expression. *, $P < .05$; **, $P < .01$. E2, 17β-estradiol.

group, the miR-1285 inhibitor and 17β-estradiol inhibited miR-1285 expression by 38.50% and 14.70%, respectively ($P < .05$-.01). Exposure to miR-1285 mimic increased miR-1285 expression by 106.80%, as compared with the mock-treated cells ($P < .01$), and weakened the inhibitory effect of 17β-estradiol on miR-1285 expression; this increased by 26.38%, as compared with the 17β-estradiol-only group ($P < .05$) (Figure 3A).

SC viability declined in the miR-1285 inhibitor-treated cells and in the 17β-estradiol-only group, by 44.35% and 37.93%, respectively, as compared with the mock group (both $P < .01$). However, treatment with miR-1285 mimic increased SC viability by 26.40% ($P < .05$) and weakened the inhibitory effect of 17β-estradiol on SC viability, which increased by 44.53% as compared with the cells exposed to 17β-estradiol only ($P < .01$) (Figure 3B). Cell cycle progression was hindered significantly in the miR-1285 inhibitor-only group and in the 17β-estradiol-only group (Figure 3C). Compared with the mock group, the miR-1285 inhibitor decreased PI and SPF by 79.30% and

Table 1. Effects of AMPK on 17 β-estradiol-regulated SC PI and SPF

Treatment	PI, %	SPF, %
Control	24.39 ± 0.28	10.50 ± 0.90
AICAR	10.39 ± 1.75[a]	3.08 ± 0.54[a]
Compound C	27.65 ± 1.22[b]	26.72 ± 1.65[a]
Compound C + E2	12.66 ± 0.88[a,c]	5.75 ± 0.56[a,c]
E2	10.68 ± 0.77[a]	4.49 ± 0.42[a]

Abbreviation: E2, 17β-estradiol. The percentages of cell numbers in the G_0/G_1, S, and G_2/M phases were detected by flow cytometry (shown in Figure 2B). Data are expressed as mean ± SD (n = 3).

[a] $P < .01$ vs control.

[b] $P < .05$ vs control.

[c] $P < .05$ vs the E2 group.

75.39%, respectively (both $P < .01$), and 17β-estradiol decreased PI and SPF by 54.93% and 53.48%, respectively (both $P < .01$). Exposure to miR-1285 mimic weakened the inhibitory effect of 17β-estradiol on cell cycle progression, with PI and SPF increased by 30.42% and 25.85%, respectively, as compared with the 17β-estradiol-only group (both $P < .05$) (Table 2).

Effects of AMPK and miR-1285 on 17β-estradiol-regulated ATP production

Compared with the control, AICAR and 17β-estradiol decreased the concentration of ATP in SCs by 55.03% and 42.09%, respectively (both $P < .01$). Compound C had no significant effect on the concentration of ATP ($P > .05$) but reduced 17β-estradiol-mediated inhibition of ATP production; this increased by 52.16%, as compared with the 17β-estradiol-only group ($P < .01$) (Figure 4A). The miR-1285 inhibitor and 17β-estradiol reduced the production of ATP in SCs by 47.13% and 31.20%, respec-

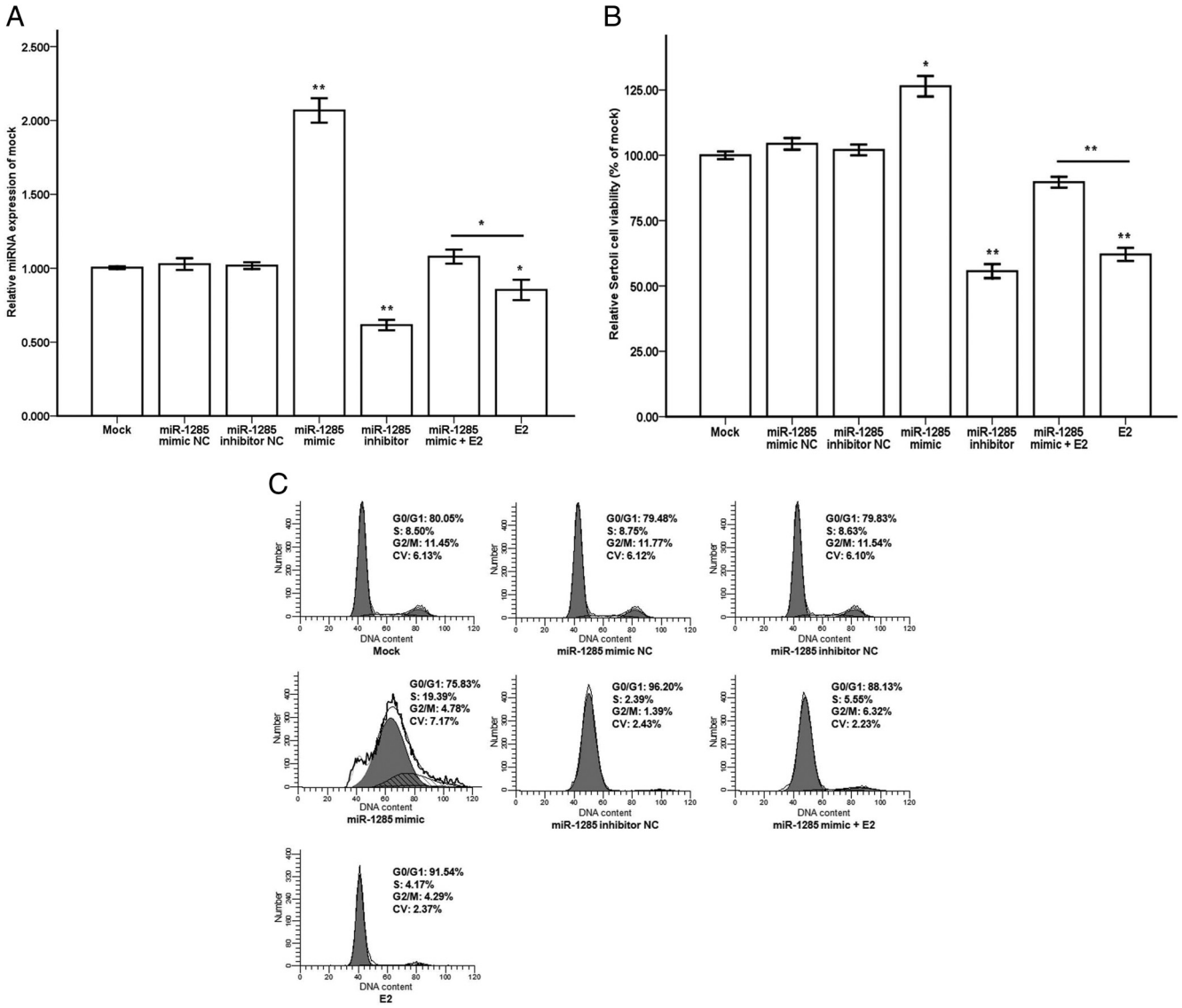

Figure 3. Effects of the miR-1285 mimic and inhibitor on 17β-estradiol-regulated expression of miR-1285, SC viability, and the cell cycle. A, Real-time-PCR analysis of miR-1285, relative to U6 expression. B, Cell viability was determined by cell counting kit-8. C, Flow cytometric analysis of the cell cycle. *, $P < .05$; **, $P < .01$. E2, 17β-estradiol.

Table 2. Effects of miR-1285 on 17 β-estradiol-regulated SC PI and SPF

Treatment	PI, %	SPF, %
Mock	21.30 ± 1.30	8.90 ± 0.35
miR-1285 mimic NC	21.92 ± 1.10	9.13 ± 0.33
miR-1285 inhibitor NC	21.67 ± 1.20	9.01 ± 0.33
miR-1285 mimic	25.17 ± 0.88[a]	18.46 ± 0.83[b]
miR-1285 inhibitor	4.41 ± 0.54[b]	2.19 ± 0.26[b]
miR-1285 mimic + E2	12.52 ± 0.58[b,c]	5.21 ± 0.26[b,c]
E2	9.60 ± 0.14[b]	4.14 ± 0.29[b]

Abbreviation: E2, 17β-estradiol. The percentages of cell numbers in the G_0/G_1, S, and G_2/M phases were detected by flow cytometry (shown in Figure 3C). Data are expressed as mean ± SD (n = 3).

[a] $P < .05$ vs mock.

[b] $P < .01$ vs mock.

[c] $P < .05$ vs the E2 group.

tively, as compared with the miR-1285 mimic NC group (both $P < .01$). However, the concentration of ATP increased by 26.07% in the cells exposed to miR-1285 mimic only ($P < .05$) and weakened the effect of 17β-estradiol on the ATP level, as compared with the 17β-estradiol-only group ($P < .01$) (Figure 4B).

Effects of AMPK and miR-1285 on 17β-estradiol regulation of AMPK and mTOR phosphorylation and p53, p27, and Skp2 expression in SCs

Compared with the control, AICAR and 17β-estradiol activated AMPK phosphorylation and increased the expression of p53 and p27 but significantly inhibited mTOR phosphorylation and Skp2 expression ($P < .05$-.01) (Figure 5, A–C). Conversely, compound C reduced the levels of phosphorylated AMPK and mTOR (both $P < .05$) (Figure 5, A and B) and had no significant effects on the expression of p53, p27, and Skp2, as compared with the control (all $P > .05$) (Figure 5C). Compound C attenuated the effects of 17β-estradiol on the phosphorylation of AMPK and mTOR and on the expression of p53 and Skp2 ($P < .05$-.01) (Figure 5, A–C).

miR-1285 mimic reduced AMPK phosphorylation and enhanced mTOR phosphorylation ($P < .05$-.01) (Figure 5, D and E). In addition, miR-1285 mimic inhibited p53 and p27 expression (by 41.78% and 53.38%, respectively), as compared with the miR-1285 mimic NC group (both $P < .05$) (Figure 5F), whereas Skp2 expression was increased by 5.66% ($P > .05$) (Figure 5F). Exposure to miR-1285 mimic reduced the effects of 17β-estradiol on the phosphorylation of AMPK and mTOR and on the expression of p53, p27, and Skp2 (all $P < .01$) (Figure 5, D–F). However, the miR-1285 inhibitor and 17β-estradiol increased AMPK phosphorylation by 31.24% and 26.34%, respectively, as compared with the miR-1285 mimic NC group (both $P < .01$) (Figure 5D). The miR-1285 inhibitor and 17β-estradiol reduced mTOR phosphorylation by 68.60% and 60.47%, respectively, as compared with the miR-1285 mimic NC group (both $P < .01$) (Figure 5E). Furthermore, the miR-1285 inhibitor and 17β-estradiol significantly enhanced the expression of both p53 (by 1.02-fold and 0.96-fold, respectively) and p27 (by 1.88-fold and 1.82-fold, respectively; all $P < .01$; Figure 5F) but inhibited Skp2 expression by 86.09% and 77.27%, respectively, as compared with the miR-1285 mimic NC group (both $P < .01$) (Figure 5F).

Effects of AMPK and miR-1285 on 17β-estradiol-mediated effects on AMPK mRNA and Skp2 mRNA in SCs

Compared with the control, AICAR and 17β-estradiol increased the levels of *AMPK* mRNA but reduced *Skp2* mRNA expression ($P < .05$-.01). Compound C reduced the levels of *AMPK* mRNA by 20.22%, increased *Skp2* mRNA levels by 37.67%, and weakened the effects of

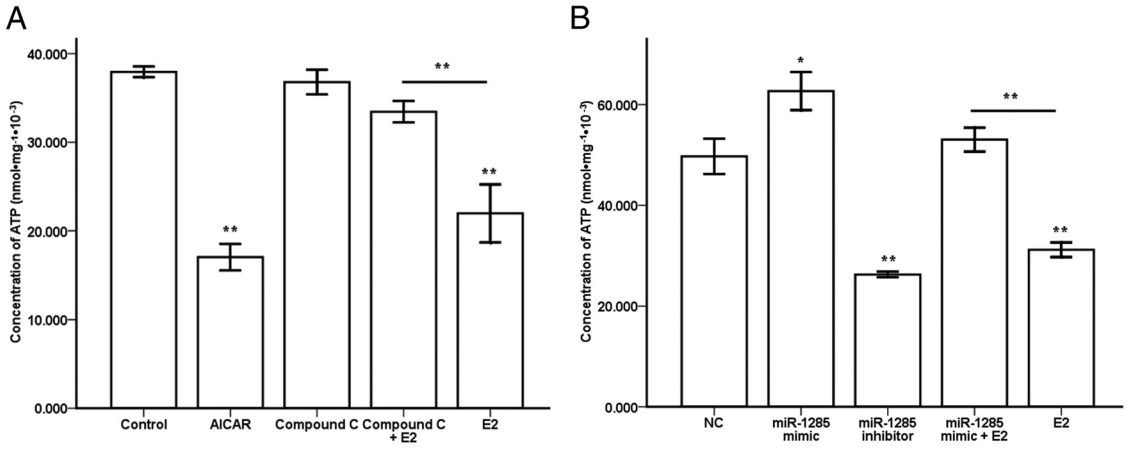

Figure 4. Effects of AMPK and miR-1285 on 17β-estradiol-mediated regulation of ATP concentrations in SCs. A, Effects of AMPK on 17β-estradiol-regulated ATP concentrations in SCs. B, Effects of miR-1285 on 17β-estradiol-regulated ATP concentrations in SCs. miR-1285 mimic negative control is simplified as NC. ATP levels were determined using a commercially available ATP kit. *, $P < .05$; **, $P < .01$. E2, 17β-estradiol.

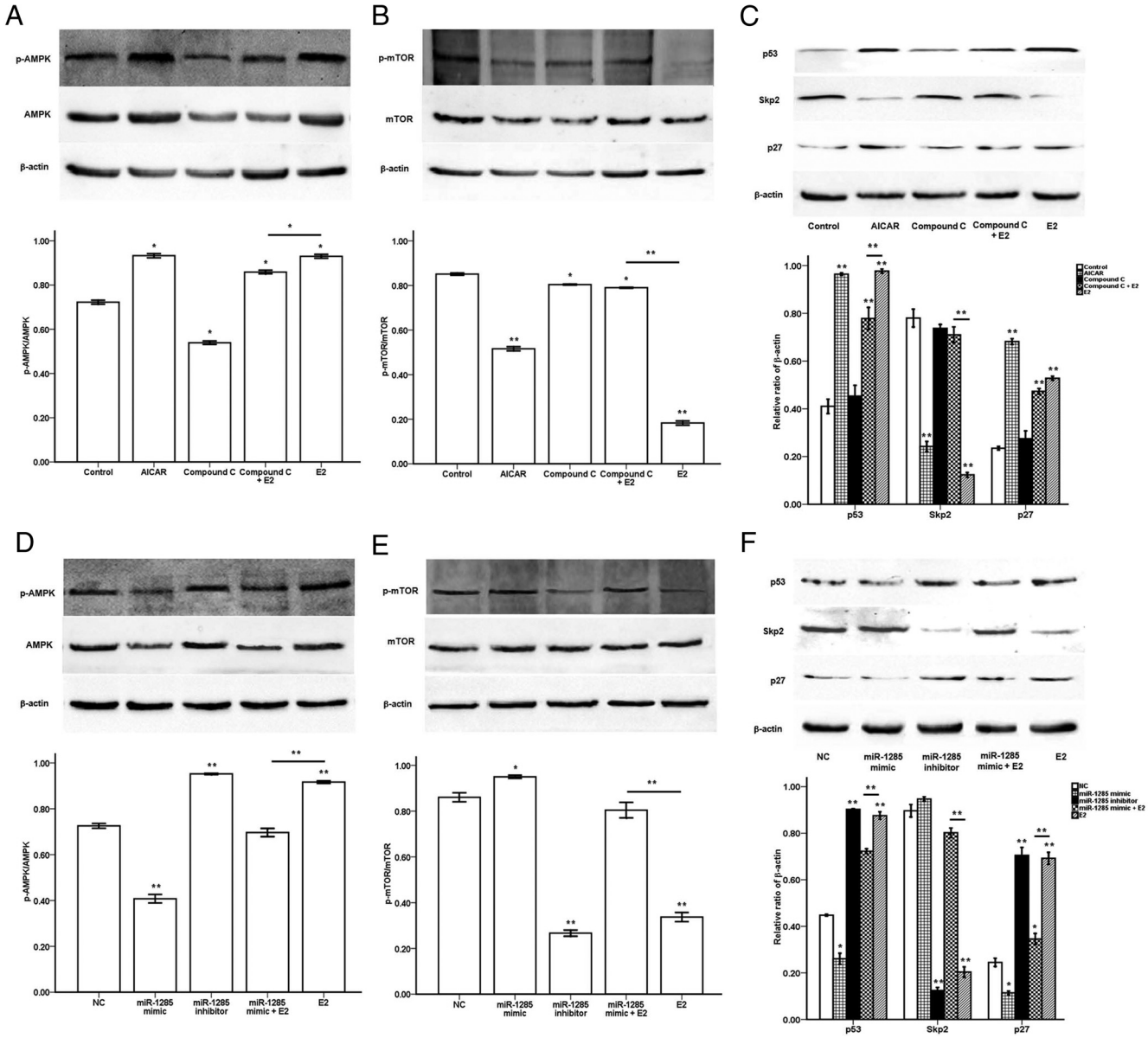

Figure 5. Effects of AMPK and miR-1285 on 17β-estradiol-regulated phosphorylation of AMPK and mTOR and on expression of p53, p27, and Skp2 in SCs. Effects of AMPK on 17β-estradiol-regulated expression of p-AMPK (A), p-mTOR (B), and p53, Skp2, and p27 (C). Effects of miR-1285 on 17β-estradiol modulation of p-AMPK (D), p-mTOR (E), and p53, Skp2, and p27 (F). *, $P < .05$; **, $P < .01$. E2, 17β-estradiol.

17β-estradiol on mRNA levels of *AMPK* and *Skp2* ($P <$ .05-.01) (Figure 6A). The miR-1285 inhibitor and 17β-estradiol increased *AMPK* mRNA expression, as compared with the miR-1285 mimic NC group, whereas *Skp2* mRNA expression was reduced ($P <$ .05-.01). miR-1285 mimic inhibited *AMPK* mRNA expression but up-regulated *Skp2* mRNA expression by 38.92% (both $P <$ .01). Furthermore, miR-1285 mimic weakened the effects of 17β-estradiol on the levels of *AMPK* mRNA and *Skp2* mRNA, whereby *AMPK* mRNA expression decreased by 32.98%, whereas *Skp2* mRNA expression increased by 49.33%, as compared with the 17β-estradiol-only group (both $P <$ .01) (Figure 6B).

Discussion

Estrogens play an important role in regulating SC proliferative capacity (8, 10, 27). The present study found that a high concentration of 17β-estradiol (10 μM) inhibited SC viability. Our results also showed that 17β-estradiol enhanced the activation of AMPK by inhibiting the expression of miR-1285. Furthermore, the AMPK activator, AICAR, and the miR-1285 inhibitor reduced mTOR phosphorylation and Skp2 expression and enhanced the expression of p53 and p27. In contrast, the AMPK inhibitor, compound C, and the miR-1285 mimic attenuated the effects of 17β-estradiol on these parameters. These

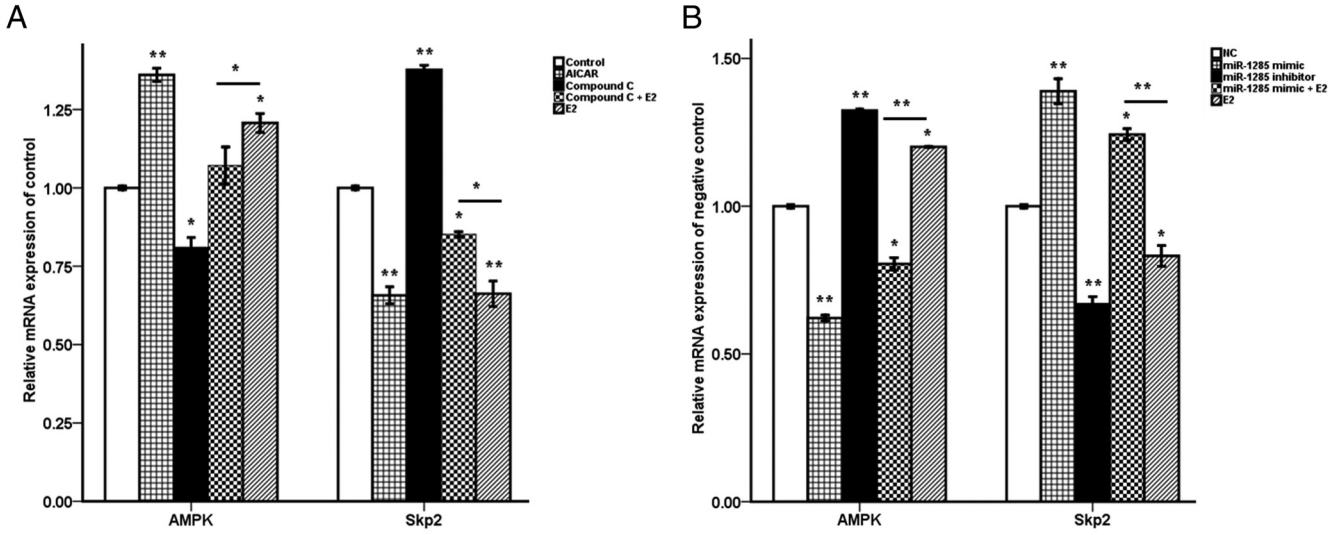

Figure 6. Effects of AMPK and miR-1285 on 17 β-estradiol-associated changes in *AMPK* and *Skp2* mRNA levels. A, Effects of AMPK on 17β-estradiol-regulated expression of *AMPK* mRNA and *Skp2* mRNA. B, Effects of miR-1285 on 17β-estradiol-regulated expression of *AMPK* mRNA and *Skp2* mRNA. The *AMPK* and *Skp2* mRNA levels were determined by real-time-PCR, and expressed relative to the *β-actin* mRNA level. *, $P < .05$; **, $P < .01$. E2, 17β-estradiol.

observations suggested that high concentrations of 17β-estradiol reduced SC viability by inhibiting the expression of miR-1285, which leads to activated AMPK; this regulates the expression of mTOR, p53, p27, and Skp2.

Different levels of estrogens have been shown to have different effects on SC proliferation, both in vitro and in vivo. The level of estradiol is about 0.6 ng/mg protein in the 6-week-old boar testes and about 1.55 ng/mg protein in the 20-week-old testes. Reducing endogenous estrogens in the postnatal interval increases the number of SCs (8). Our previous results showed that 17β-estradiol (0.0001–0.1 μM) increased the number of immature boar SCs in vitro, whereas 1 μM 17β-estradiol reduced the number of SCs (10). Similarly, in vivo inhibition of estrogen synthesis in boars aged 6.5 weeks reduced estradiol levels to 0.05 ng/mg protein by letrozole treatment and increased the numbers of SCs (30). In this study, we demonstrated that the inhibitory effects of 17β-estradiol on SC viability were enhanced as the dose and duration of exposure increased. The effect of estrogens on cell proliferation capacity is affected by the stage of physiological development. SCs produce a certain amount of estrogens, which promote cell proliferation during the first 2 months of life (31). However, estradiol benzoate suppressed SC proliferation during puberty, resulting in increased SC apoptosis (9). We therefore hypothesize that estrogens activate a mechanism resulting in negative regulation of cell proliferation in SCs.

AMPK negatively regulates cell proliferation. Activated AMPK inhibits the proliferation of the GH3 pituitary tumor cell line (32) and estrogen receptor-positive breast carcinoma cells (33). AMPK activation also decreases in S6K phosphorylation and FSH-stimulated SC proliferation via the phosphoinositol 3-kinase/alanine aminotransferase/mTOR complex 1 signaling pathway. These observations led to speculation that AMPK regulates the transition of SCs from the mitotic to the postmitotic state (34). In this study, we showed that 10 μM 17β-estradiol inhibited immature boar SC viability and cell cycle progression by activating the AMPK signaling pathway. Furthermore, AICAR inhibited SC viability, whereas compound C enhanced SC viability, indicating that AMPK is involved in 17β-estradiol-mediated reduction of SC viability. Estrogens affect cell proliferation and energy metabolism (35). Our observations demonstrated that AICAR, 17β-estradiol, and the miR-1285 inhibitor reduced the concentration of ATP, whereas compound C and miR-1285 mimic weakened the effects of 17β-estradiol. We found that AICAR significantly decreased the ATP concentration; this was inconsistent with some literature indicating that AICAR had no effect or a slight increase on the ATP concentration. This difference may relate to the duration of AICAR exposure. A short treatment with AICAR did not affect or slightly increased cellular ATP content (36, 37), whereas AICAR infusion for 90 minutes elicited a significant reduction in ATP levels, resulting in a 3-fold rise in the AMP to ATP ratio (38). Our study showed that both AICAR and 17β-estradiol inhibited the expression of miR-1285, whereas compound C increased miR-1285 expression and weakened the effects of 17β-estradiol on miR-1285. Furthermore, miR-1285 inhibitor activated AMPK, and miR-1285 mimic weakened the effects of 17β-estradiol on the phosphorylation of AMPK. Therefore, we conclude that 17β-estradiol reduced the expression of miR-1285, resulting in AMPK

activation, which decreased the ATP concentration. Our results indicate that estrogens inhibit SC proliferation capacity by inhibiting the expression of miR-1285. Although miR-1285 inhibited p53 expression by direct binding to the 3′-UTR in human embryonic kidney 293T cells (39), our previous study showed that p53 was not the target gene of miR-1285 in boar SCs (Zhang J.J., Wang Y., Yang W.R., Jeong D.K., Wang X.Z., unpublished data). Our results therefore rule out the possibility that miR-1285 inhibits cell proliferation by increasing the expression of p53.

Activated AMPK regulates cell proliferation in many ways. First, activated AMPK inhibits mTOR signaling and cell proliferation (19). In the present study, we showed that AICAR, the miR-1285 inhibitor, and 17β-estradiol inhibited mTOR phosphorylation, whereas compound C and miR-1285 mimic weakened the inhibitory effect of 17β-estradiol on mTOR phosphorylation. The potential mechanisms by which AMPK regulates mTOR phosphorylation include phosphorylation of tuberous sclerosis complex 2 at Thr1227 and Ser1345, direct phosphorylation of mTOR at Thr2446 (40), regulation of kinases downstream of mTOR, and dephosphorylation of 4E binding protein 1 and S6K1 (19, 40). Second, activated AMPK regulates the expression of p53, p27, and Skp2. Activated AMPK inhibited the proliferation of cancer cells both in vitro and in vivo by increasing p53 and p27 (20), whereas the depletion of AMPK in mouse vascular smooth muscle cells increased cell proliferation by up-regulating Skp2 expression and down-regulating p27 expression (41). We found that activated AMPK enhanced the expression of p53 and p27 but inhibited the expression of Skp2 at both the mRNA and protein levels. Compound C weakened the effects of 17β-estradiol on p53, p27, and Skp2. The mechanism involved in these effects involves AMPK-mediated p53 and p27 accumulation, which maintain low phosphorylation of retinoblastoma tumor suppressor protein. This inhibits expression of Skp2 and cyclin E, inducing cell cycle arrest (20, 42, 43). p53 decreases the expression of Skp2 (44), and Skp2 controls the late G_1 and S phase degradation of p27 (42), indicating the existence of the p53-Skp2-p27 regulatory pathway in cell cycle progression. On the other hand, the mTOR inhibitor, rapamycin, decreases Skp2 expression, and the RNA interference-mediated Skp2 silencing in human tumor cells enhances their sensitivity to rapamycin in vitro, resulting in the inhibition of the growth of transplanted tumors in vivo (45). These results suggest that Skp2 is the downstream integration point of p53 and mTOR. Therefore, it can be speculated that AMPK inhibits SC proliferation via the p53 and mTOR signal pathways; these converge at Skp2, which, in turn, regulates p27 levels.

Conclusions

High concentrations of 17β-estradiol exert a negative influence on SC proliferation by inhibiting miR-1285 expression. This activates AMPK by reducing the ATP concentration and increasing the expression of *AMPK* mRNA. Phosphorylated AMPK up-regulates the expression of p53 and p27 and inhibits the expression of mTOR and Skp2. In addition, our data indicate that Skp2 is the downstream integration point of p53 and mTOR and regulates the expression of p27. These results elucidate the mechanism by which 17β-estradiol negatively regulates spermatogenesis and highlight the involvement of miR-1285 in the control of SC number and sperm production in boars.

Acknowledgments

We are thankful to the China Scholarship Council for providing a scholarship fund to the first author.

Address all correspondence and requests for reprints to: Wang Xian Zhong, PhD, Professor, College of Animal Science and Technology, Southwest University, Chongqing, 400715, China. E-mail: xianzhong_wang@aliyun.com.

This work was supported by grants from the National Natural Science Foundation of China (Grant 31072183), the Major State Basic Research Development Program (Grant 2014CB138502), and the Next-Generation BioGreen 21 Program (Grant PJ01117401), Rural Development Administration, Republic of Korea.

Disclosure Summary: The authors have nothing to disclose.

References

1. **Rato L, Alves MG, Socorro S, Duarte AI, Cavaco JE, Oliveira PF.** Metabolic regulation is important for spermatogenesis. *Nat Rev Urol*. 2012;9:330–338.
2. **Oliveira PF, Sousa M, Barros A, Moura T, Rebelo da Costa A.** Intracellular pH regulation in human Sertoli cells: role of membrane transporters. *Reproduction*. 2009;137:353–359.
3. **Smith BE, Braun RE.** Germ cell migration across Sertoli cell tight junctions. *Science*. 2012;338:798–802.
4. **Franca LR, Silva VA Jr, Chiarini-Garcia H, Garcia SK, Debeljuk L.** Cell proliferation and hormonal changes during postnatal development of the testis in the pig. *Biol Reprod*. 2000;63:1629–1636.
5. **Mruk DD, Cheng CY.** Sertoli-Sertoli and Sertoli-germ cell interactions and their significance in germ cell movement in the seminiferous epithelium during spermatogenesis. *Endocr Rev*. 2004;25:747–806.
6. **Dorrington JH, Bendell JJ, Khan SA.** Interactions between FSH, estradiol-17β and transforming growth factor-β regulate growth and differentiation in the rat gonad. *J Steroid Biochem Mol Biol*. 1993;44:441–447.
7. **Kao E, Villalon R, Ribeiro S, Berger T.** Role for endogenous estrogen in prepubertal Sertoli cell maturation. *Anim Reprod Sci*. 2012;135:106–112.

8. **Berger T, Conley AJ.** Reducing endogenous estrogen during prepubertal life does not affect boar libido or sperm fertilizing potential. *Theriogenology*. 2014;82:627–635.
9. **Walczak-Jedrzejowska R, Slowikowska-Hilczer J, Marchlewska K, Kula K.** Maturation, proliferation and apoptosis of seminal tubule cells at puberty after administration of estradiol, follicle stimulating hormone or both. *Asian J Androl*. 2008;10:585–592.
10. **Wang X-Z, Zhao B-C, Zhou Y-L, Zhou Y-T, Ma K-G, Zhang J-H.** 17β-Estradiol regulates cultured immature boar Sertoli cell proliferation via the cAMP-ERK1/2 pathway and the estrogen receptor β. *Agric Sci China* 2010;9:1201–1210.
11. **Bode AM, Dong Z.** Post-translational modification of p53 in tumorigenesis. *Nat Rev Cancer*. 2004;4:793–805.
12. **Johnson SC, Rabinovitch PS, Kaeberlein M.** mTOR is a key modulator of ageing and age-related disease. *Nature*. 2013;493:338–345.
13. **Liu L, Luo Y, Chen L, et al.** Rapamycin inhibits cytoskeleton reorganization and cell motility by suppressing RhoA expression and activity. *J Biol Chem*. 2010;285:38362–38373.
14. **Imamura K, Ogura T, Kishimoto A, Kaminishi M, Esumi H.** Cell cycle regulation via p53 phosphorylation by a 5′-AMP activated protein kinase activator, 5-aminoimidazole-4-carboxamide-1-β-D-ribofuranoside, in a human hepatocellular carcinoma cell line. *Biochem Biophys Res Commun*. 2001;287:562–567.
15. **Jones RG, Plas DR, Kubek S, et al.** AMP-activated protein kinase induces a p53-dependent metabolic checkpoint. *Mol Cell*. 2005;18:283–293.
16. **Igata M, Motoshima H, Tsuruzoe K, et al.** Adenosine monophosphate-activated protein kinase suppresses vascular smooth muscle cell proliferation through the inhibition of cell cycle progression. *Circ Res*. 2005;97:837–844.
17. **Fan J, Yang X, Bi Z.** 6-Gingerol inhibits osteosarcoma cell proliferation through apoptosis and AMPK activation. *Tumour Biol*. 2015;36(2):1135–1141.
18. **Wang Y, Liu W, He X, Fei Z.** Hispidulin enhances the anti-tumor effects of temozolomide in glioblastoma by activating AMPK. *Cell Biochem Biophys*. 2015;71(2):701–706.
19. **Kimura N, Tokunaga C, Dalal S, et al.** A possible linkage between AMP-activated protein kinase (AMPK) and mammalian target of rapamycin (mTOR) signalling pathway. *Genes Cells*. 2003;8:65–79.
20. **Rattan R, Giri S, Singh AK, Singh I.** 5-Aminoimidazole-4-carboxamide-1-β-D-ribofuranoside inhibits cancer cell proliferation in vitro and in vivo via AMP-activated protein kinase. *J Biol Chem*. 2005;280:39582–39593.
21. **Kahn BB, Alquier T, Carling D, Hardie DG.** AMP-activated protein kinase: ancient energy gauge provides clues to modern understanding of metabolism. *Cell Metab*. 2005;1:15–25.
22. **Nicholls PK, Harrison CA, Walton KL, McLachlan RI, O'Donnell L, Stanton PG.** Hormonal regulation of Sertoli cell micro-RNAs at spermiation. *Endocrinology*. 2011;152:1670–1683.
23. **Piriyapongsa J, Marino-Ramirez L, Jordan IK.** Origin and evolution of human microRNAs from transposable elements. *Genetics*. 2007;176:1323–1337.
24. **Filshtein TJ, Mackenzie CO, Dale MD, et al.** OrbId: Origin-based identification of microRNA targets. *Mobile Genet Elements*. 2012;2:184–192.
25. **Morin RD, O'Connor MD, Griffith M, et al.** Application of massively parallel sequencing to microRNA profiling and discovery in human embryonic stem cells. *Genome Res*. 2008;18:610–621.
26. **Spengler RM, Oakley CK, Davidson BL.** Functional microRNAs and target sites are created by lineage-specific transposition. *Hum Mol Genet*. 2014;23:1783–1793.
27. **Lucas TF, Siu ER, Esteves CA, et al.** 17β-Estradiol induces the translocation of the estrogen receptors ESR1 and ESR2 to the cell membrane, MAPK3/1 phosphorylation and proliferation of cultured immature rat Sertoli cells. *Biol Reprod*. 2008;78:101–114.
28. **Guan S, Ge D, Liu TQ, Ma XH, Cui ZF.** Protocatechuic acid promotes cell proliferation and reduces basal apoptosis in cultured neural stem cells. *Toxicol In Vitro*. 2009;23:201–208.
29. **Livak KJ, Schmittgen TD.** Analysis of relative gene expression data using real-time quantitative PCR and the 2(-$\delta\delta$C[T]) method. *Methods*. 2001;25:402–408.
30. **Berger T, Kentfield L, Roser JF, Conley A.** Stimulation of Sertoli cell proliferation: defining the response interval to an inhibitor of estrogen synthesis in the boar. *Reproduction*. 2012;143:523–529.
31. **Ramesh R, Pearl CA, At-Taras E, Roser JF, Berger T.** Ontogeny of androgen and estrogen receptor expression in porcine testis: effect of reducing testicular estrogen synthesis. *Anim Reprod Sci*. 2007;102:286–299.
32. **Tulipano G, Faggi L, Cacciamali A, Spinello M, Cocchi D, Giustina A.** Interplay between the intracellular energy sensor AMP-activated protein kinase (AMPK) and the estrogen receptor activities in regulating rat pituitary tumor cell (GH3) growth in vitro. *Pituitary*. 2014;17:203–209.
33. **Ma J, Guo Y, Chen S, et al.** Metformin enhances tamoxifen-mediated tumor growth inhibition in ER-positive breast carcinoma. *BMC Cancer*. 2014;14:172.
34. **Riera MF, Regueira M, Galardo MN, Pellizzari EH, Meroni SB, Cigorraga SB.** Signal transduction pathways in FSH regulation of rat Sertoli cell proliferation. *Am J Physiol Endocrinol Metab*. 2012;302:E914–E923.
35. **Mauvais-Jarvis F, Clegg DJ, Hevener AL.** The role of estrogens in control of energy balance and glucose homeostasis. *Endocr Rev*. 2013;34:309–338.
36. **Merrill GF, Kurth EJ, Hardie DG, Winder WW.** AICA riboside increases AMP-activated protein kinase, fatty acid oxidation, and glucose uptake in rat muscle. *Am J Physiol*. 1997;273:E1107–E1112.
37. **Nguyen TM, Alves S, Grasseau I, et al.** Central role of 5′-AMP-activated protein kinase in chicken sperm functions. *Biol Reprod*. 2014;91:121.
38. **Hasenour CM, Ridley DE, Hughey CC, et al.** 5-Aminoimidazole-4-carboxamide-1-β-D-ribofuranoside (AICAR) effect on glucose production, but not energy metabolism, is independent of hepatic AMPK in vivo. *J Biol Chem*. 2014;289:5950–5959.
39. **Tian S, Huang S, Wu S, Guo W, Li J, He X.** MicroRNA-1285 inhibits the expression of p53 by directly targeting its 3′ untranslated region. *Biochem Biophys Res Commun*. 2010;396:435–439.
40. **Bartolome A, Guillen C, Benito M.** Role of the TSC1-TSC2 complex in the integration of insulin and glucose signaling involved in pancreatic β-cell proliferation. *Endocrinology*. 2010;151:3084–3094.
41. **Song P, Wang S, He C, Liang B, Viollet B, Zou MH.** AMPKα2 deletion exacerbates neointima formation by upregulating Skp2 in vascular smooth muscle cells. *Circ Res*. 2011;109:1230–1239.
42. **Assoian RK, Yung Y.** A reciprocal relationship between Rb and Skp2: implications for restriction point control, signal transduction to the cell cycle and cancer. *Cell Cycle*. 2008;7:24–27.
43. **Okoshi R, Ozaki T, Yamamoto H, et al.** Activation of AMP-activated protein kinase induces p53-dependent apoptotic cell death in response to energetic stress. *J Biol Chem*. 2008;283:3979–3987.
44. **Hu R, Aplin AE.** Skp2 regulates G2/M progression in a p53-dependent manner. *Mol Biol Cell*. 2008;19:4602–4610.
45. **Totary-Jain H, Sanoudou D, Dautriche CN, Schneller H, Zambrana L, Marks AR.** Rapamycin resistance is linked to defective regulation of Skp2. *Cancer Res*. 2012;72:1836–1843.